FACHHOCHSCHULE **TRIER**
Hochschule für Technik, Wirtschaft und Gestaltung
University of Applied Sciences
Informatik

Informatik-Bericht Nr. 2008-5

Schriftenreihe Fachbereich Informatik, Fachhochschule Trier

Automated Target Location And Trajectory Selection For Stereotactic Planning In Deep Brain Stimulation

P. Gemmar[1], O. Gronz, K. Fisch, P. Mrosek, F. Hertel[2], C. Decker
[1] University of Applied Sciences (FH) Trier, [2] Klinikum Idar-Oberstein GmbH, Germany
p.gemmar@fh-trier.de

Abstract. Image based target determination and trajectory planning are essential procedures for deep brain stimulation (DBS). Using techniques of digital image processing, we developed software prototypes for computer-supported DBS planning procedures. The prototypes detect automatically the anatomical landmarks AC and PC (anterior and posterior commissure of the third ventricle) in a sequence of T1-weighted magnetic resonance images (T1-MRI). For electrode implantation, they determine and assess a set of trajectories from an entry region to the target point. Image processing methods, which combine structural and morphological feature extraction, are described for determination of the mid-sagittal plane (MSP) and localization of AC and PC. Brain tissue is segmented in critical and non-critical matter and 3D cost functions are introduced for trajectory assessment. The prototypes were tested successfully with 39 T1-MRI data sets gained from different patients at various hospitals in Europe.

1 Introduction

Stereotactic deep brain stimulation (DBS) is an established treatment option for different kinds of neurological diseases, especially movement disorders, such as Parkinson's disease (PD), Dystonia or different kinds of tremors [1]. The Subthalamic Nucleus (STN) is considered to be the most promising target for DBS electrodes in the treatment of advanced PD. The STN is a small, almond-shaped structure, which is located in the midbrain, adjacent to the Substantia Nigra (SNR) and the Red Nucleus [2]. Different methods exist for the identification of the anatomical position of neural areas for DBS targeting. The STN and its boundaries are directly visible in T2-weighted magnetic resonance images (T2-MRI). However, T2-MRI can bear significant geometric inhomogeneities. Therefore, an indirect targeting method based on detection of the anatomical landmarks AC and PC (anterior and posterior commissure of the third ventricle), which can surely be recognized in T1-weighted MRI (T1-MRI), seems to be more exact. The topographical relation between ACPC-midpoint and the target STN is well known from the literature [3,4,5,6].

The preoperative planning procedure for stereotactic DBS is practically dominated by two steps: target localization and trajectory planning. First, the target position for the placement of the stimulating electrodes has to be decided. Second, a secure trajectory has to be chosen for inserting the electrode from the burr hole to the target point without intersecting critical brain tissue. Currently, this task is performed by the neurosurgeon. It requires high experience and it is also time consuming.

The aim of our study was the development of automatic methods for the DBS planning procedure. First, our system detects anatomical landmarks AC and PC and the mid-sagittal plane in a sequence of T1-MRI and calculates the target position for the DBS electrodes. In a next step, cerebral structures are analyzed in T1-MRI and classified into critical and non-critical tissue. Based on this, suitable and safe trajectories between a specified entry area and the target are calculated. The trajectories are valued by means of their risk of penetrating critical cerebral tissue and the best valued trajectories are proposed for DBS. Both methods support optimized results in a standardized manner, but the neurosurgeon must make the final decision.

2 Methods

Normal human brains exhibit an approximate bilateral symmetry, although they are not perfectly symmetrical. The plane with respect to which the brain is most symmetric is called the brain symmetry plane or the mid-sagittal plane (MSP) which separates both brain hemispheres. Exactly in MSP, the anatomical landmarks AC and PC can be identified. The midpoint between AC and PC can be used as origin of a 3D Cartesian coordinate system orthogonal with MSP. Now, the position of STN can be defined easily by its 3D distance from the origin.

Using the symmetry characteristics of the human brain, we localize the MSP in 3D T1-MRI, which are acquired as a reconstruction of sequential 2D axial T1-MRI. 3D segmentation of the third ventricle and examination of its geometric orientation are suitable means for the determination of MSP. Now, the landmarks AC and PC can be searched and recognized as bright pixels at distinguished positions on the border of the third ventricle in MSP. In order to improve image quality and to support successful segmentation of the third ventricle, the T1-MRIs should firstly be preprocessed to remove noise and artifacts.

After calculation of the target positions, we have to look for possible entry points and suitable trajectories, along which the electrodes can securely be inserted. Entry points should lie on gyri and trajectories should not pass through critical brain tissue like e.g. sulci, ventricles or blood vessels. Potential entry points can be found on the surface of the brain in a preselected entry region. Segmentation of the whole brain followed by 3D contour extraction delivers a set of entry points. All trajectories from the set of entry points to the target can be valued according to how near they pass critical tissue. T1-MRI values of critical tissue differ from values of gray or white matter, and segmentation of brain tissue in critical or non-critical areas can be based on this comparison. Finally, the best valued trajectories can be suggested to the surgeon, who has to decide which should be used at last.

We used 14 T1-MRI patient data sets from the Hospital of the Merciful Brethren in Trier, Germany, and another 25 patient data sets from various hospitals in Europe. Pixel spacing ranged from 0.625mm to 1.07mm and image resolution was mainly 256×256, a few data sets used 512×512. Slice thickness ranged from 1 mm to 2mm. For testing of system accuracy, we only considered data sets with slice thickness not larger than 1.5mm. Slice thickness and distance between slices must also fit.

2.1 AC/PC Localization

It is essential for correct detection of AC and PC to rely on an optimal segmentation of the third ventricle. Supporting this goal, preprocessing of T1-MRI should reduce noise and artifacts. We use a nonlinear anisotropic diffusion (NLAD) filter for image enhancement in T1-MRI [7]. NLAD works similarly to a physical diffusion process on gradients of voxel (volume element) values and removes noise while preserving edges. The diffusion theory in imaging raised from an analogy with fluids diffusion. It states that the image intensity u, analogous to a fluid concentration, is evolving towards an equilibrium state. Nonlinear anisotropic models combine two features: non-linearity effectuates that diffusion at borders is reduced or stopped and anisotropy leads to the effect, that diffusion should be perpendicular to edges and that there is no diffusion over edges. The model can be described by the diffusion equation

$$\frac{\partial u}{\partial t} = \nabla(D\nabla u)$$

where D is the diffusion tensor, a positive symmetric matrix, and t denotes the diffusion time. The diffusion equation is often put in discrete form by explicit schemes. But those schemes are only stable for very small time steps and lead to poor efficiency. Therefore, we used the optimized *additive operator splitting* (AOS) scheme that is described in [7,8]. The advantage

of this strategy is that it is stable for many time steps and it can be applied to n-dimensional problems. AOS-schemes are at least ten times more efficient than explicit schemes.

Next, we segment the third ventricle as a set of connected voxels according to a prescribed criterion. In the context of 3D-segmentation, region growing (RG, [9]) and geometric (implicit) active contour models (GACM, [10,11]) are promising techniques to extract a connected region like the third ventricle from a 3D volume. In order to achieve optimal border information of the third ventricle for AC and PC localization, these segmentation methods were tested. Finally, we used a modified 3D region growing algorithm for this task (see Fig. 1). The growing starts from a seed point set interactively in the third ventricle. Then the gray value distances of the six immediate neighbors of that voxel are calculated. The distance is a simple measure of how much the intensity *g(x,y,z)* of the regarded voxel differs from the mean intensity value μ of the voxels from the region already segmented. If the distance rises above a threshold θ, the voxel is not attached to the region. The homogeneity function h is then

$$h(x,y,z) := \begin{cases} 1, & |g(x,y,z) - \mu| \le \theta \\ 0, & \text{otherwise} \end{cases}.$$

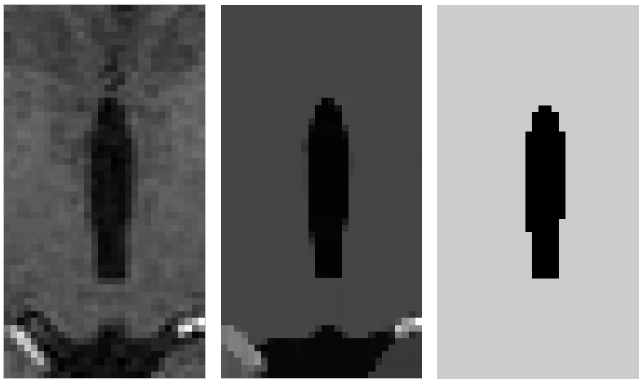

Fig 1. Segmentation of third ventricle; left: original region of interest (axial view), middle: result of NLAD-filtering; right: segmented

Since the whole human brain shows approximately a symmetrical anatomy, we consider the bilateral symmetry plane of the third ventricle for locating of the MSP. The symmetry axis of the third ventricle is detected by 3D skeletonizing of the segmented ventricle. Using iterative and successive binary thinning [9], this morphological operation generates a minimally connected line that is equidistant from the boundaries of the ventricle. Applying this method to every axial T1-MRI, a plane in the 3D space is constructed which forms the MSP.

During the T1-MRI exposure, the patient's head is not fixed. Depending upon the patient's position in the MR tomograph, the head can be tilted differently in each direction. In order to extract the orientation of MSP, the possible inclination angles have to be calculated so that the T1-MRI can be aligned uniformly. The only relevant inclination angles are the axial angle α and the coronal angle β. The inclination angles of the MSP can be calculated by projecting the MSP skeleton profile onto the according coordinate planes. Doing so, we get projection lines, which we approximate to straight lines by usage of the Hough transform. In standard Hough transform, each line in a 2D coordinate system is represented by the angle φ between the line's normal and the abscissa, and its distance ρ from the origin. The angle φ corresponds to the inclination angle of the patient's head in the coordinate plane considered actually. Applying this method to the axial and coronal projection of the mid-sagittal skeleton plane, both the axial inclination angle α and the coronal inclination angle β can be calculated (see Fig. 2). Then, the whole T1-MRI sequence is rotated by the calculated angles using bicubic

interpolation. Each target pixel value is generated by interpolation from values from sixteen source pixels mapped as nearest. This algorithm yields a good balance between detail preservation and smoothness.

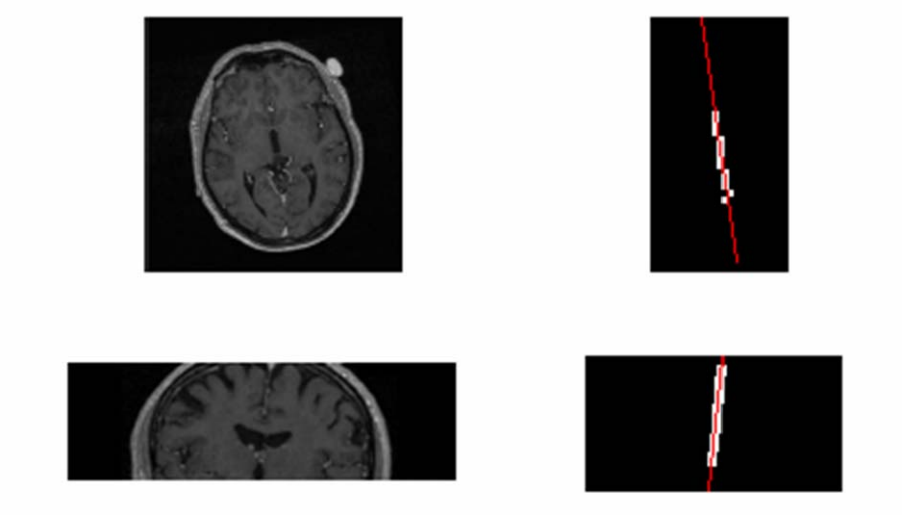

Fig 2. Calculation of the axial inclination angle α (above) and coronal angle β (below); left: T1-MRI of an inclined head; right: projected skeleton lines (white) and Hough lines (red) of the third ventricle

After extracting MSP, landmarks AC and PC can be identified at the anterior and posterior boundaries of the third ventricle (see Fig. 3). The AC is a bundle of nerve fibers that forms the cross connection between the two hemispheres [12]. In the MSP, AC is located immediately inferior to the column of fornix. In T1-MRI, bundles of nerve fibers appear as pixels with high intensity values. Thus, landmark AC can be recognized as the brightest pixel at the front contour of the third ventricle. The PC is a large fiber bundle that crosses the midline of the epithalamus just dorsal to the point where the cerebral aqueduct (CA) opens into the third ventricle. Due to the fact that the CA cannot be identified exactly in the previous 3D-segmentation result, we used a histogram-based threshold method for segmentation of the details of the CA [13]. Now, we can localize the nerve bundle of PC by using a specialized contour following method regarding its geometric position within the segmented area.

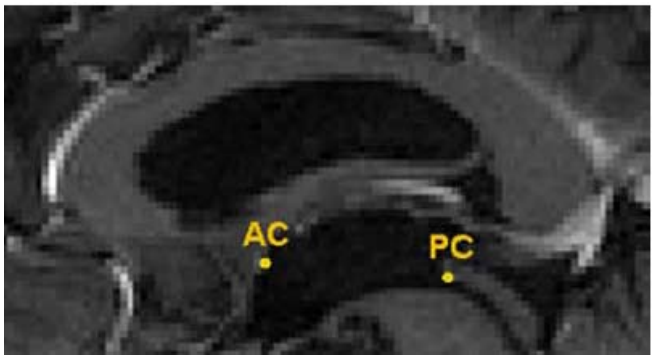

Fig 3. Localization of AC and PC on the borders of third ventricle and cerebral aqueduct

2.2 Trajectory Selection

We use NLAD-filtering (see previous section) for preprocessing of T1-MRI in order to get homogeneous representations of white and gray matter. 3D smoothing is achieved by applying this 2D filter slice per slice in all three directions (axial, sagittal, coronal) of the discrete volume data. Next, we segment white and gray matter from the remaining material

using 3D RG (see previous section). RG starts with a seed point interactively selected in gray matter at an arbitrary position and T1-MRI slice. RG considers six nearest neighbors in 3D and only attaches voxels to the segmented region, the values of which deviate less than a defined amount from the value of the seed point.

In a next step, all potential entry points for trajectories are extracted within an entry region, which is typically defined with respect to medical and cosmetic points of view. It is recommended that the entry points should lie on a gyrus, whereas sulci should be avoided. Therefore, we extract the 3D surface of the brain and select the set of all surface points within the entry region not lying in a sulcus. Principally, we expect the entry points lying on the 3D contour C of the brain. Having the segmented brain S, we determine the contour C by the use of morphologic image operations [9]. First, we close segmentation gaps and smooth the outer contour of S by the following morphologic closing operation:

$$S_c = ((S \oplus X) \Theta X) \ .$$

We use a 3D structuring element X of spherical shape for morphologic operations dilation $\oplus$ and erosion Θ, which are performed sequentially. The discrete contour C can simply be extracted from segmentation S by subtraction of the eroded segmentation S':

$$C = S - S' = S - (S \Theta X) \ .$$

Contour points lying close to the bony arch of the skull are considered for potential entry points not lying in a sulcus. So, we define the set C_E of allowed entry points $P=(x,y,z)$ as all contour points having a distance D to the skull bone smaller than a threshold ΔD (see Fig. 4):

$$C_E := \{P \mid P \in C \wedge (D(P, S_C) < \Delta D)\} \ .$$

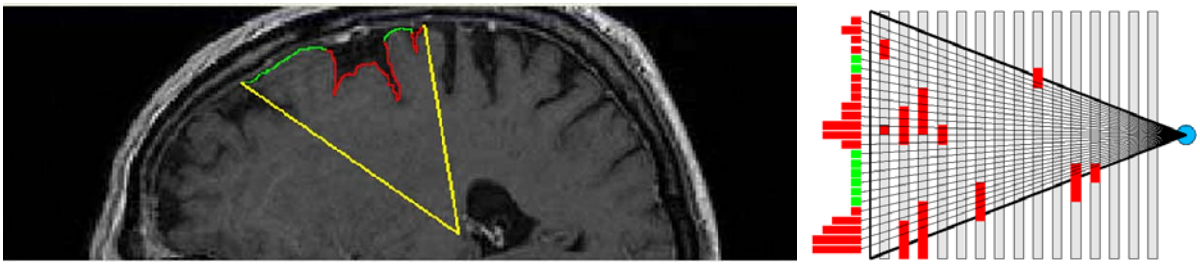

Fig 4. Selection of entry points and trajectories; left accepted (green) and rejected entry points in entry funnel (yellow); right: critical areas in any T1-MRI slices and rejected trajectories (red)

Quality and usability of possible trajectories are assessed by two methods. First, trajectories are rejected that intersect critical tissue. For every voxel lying in a critical area in the funnel of the entry region and in any T1-MRI slice, we calculate a straight line from the target point through this voxel. This straight line intersects contour C and each potential entry point P is eliminated that is hit by the straight line (see Fig. 4, right). Second, trajectories t_i from the remaining entry points to the target are valued by using a local cost function. Every trajectory t_i intersects the brain volume in 2D T1-MRI slices s_j at position P_j. We define a 2D neighborhood N_j (e.g. 7×7 voxel matrix Q_{rs} with center voxel P_j) and compare all the T1-MRI values $g(Q_{rs})$ with an average value g_a representing non-critical brain tissue. g_a can be determined from the T1-MRI histogram of segmented brain tissue, and the assumption that e.g. more than 80% of the distribution bins are produced by gray or white matter. Then, the absolute differences $|g_a\text{-}g(Q_{rs})|$ are weighted exponentially by weights representing the distance $D(Q_{rs},P_j)$. The local weights are defined by a cost matrix M_{rs}, which has the same size as neighborhood N_j. Finally, the trajectories t_i are valued by the sum of their local costs calculated over all slices s_j. The accepted trajectories are ranked according to their total cost assessment and the best n trajectories are suggested to the surgeon.

3 Results

Both methods were developed and implemented as software prototypes with Matlab™. The prototypes were tested with 39 T1-MRI data sets gained from different patients at various hospitals in Europe. AC and PC were detected correctly with a maximum difference of one pixel in more than 90% of the cases. Statistical values of AC/PC detection are shown in Tab.1. System accuracy lies within the range of the geometric resolution of the T1-MRI data used.

	AC			PC		
	Δx	Δy	Δz	Δx	Δy	Δz
Mean	0.5	1.82	0.97	0.41	0.48	0.32
Standard deviation	0.6	3.71	1.84	0.47	1.56	0.71

Tab 1. Mean and standard deviation (in mm) of automatic AC/PC detection

For trajectory planning, the system proposed a set of trajectories for each calculated target, of which at least 4 or 5 trajectories were accepted for DBS by an experienced neurosurgeon. The remaining data sets (< 10%) were not correctly classified due to major anatomical variations or because of poor image quality.

4 Discussion

The prototypes calculated correctly the coordinates of AC and PC, as well as the MSP for 32 out of 39 patient data sets. In 2 cases the software delivered wrong results. For 5 data sets the software could not come out with correct results, due to anatomic variations or low MRI quality. The average absolute difference was less than 1 mm for accepted AC/PC coordinates compared to those which were determined manually. That means, the accuracy of the automatic determination system lies within the range of the geometric resolution (pixel size) of the MRI data used.

Trajectory planning worked well for all patient data sets of which AC/PC detection provided correct information for calculation of target coordinates. For all targets, at least five trajectories were suggested and accepted by an experienced neurosurgeon.

The computational processing time averaged to less than 15 seconds for the determination of the AC/PC coordinates and to less than 5 minutes for trajectory planning. Processing was performed for data sets consisting of 90 T1-MRI slices with 256×256 pixels on a standard PC with 1,6 GHz Intel Pentium IV CPU and 512 MB RAM.

5 Conclusion

We can conclude, that the software system calculates successfully intercommissural AC/PC-line for T1-MRI data with good quality and brain tissues without abnormal anatomic structures. In the case of errors, the deviation of AC/PC coordinates is evident at least in one coordinate axis, so it can be recognized easily and can also be monitored by the length of the intercommissural AC/PC-line. Segmentation of brain tissue was soundly and the qualification of critical and non-critical always delivered suitable results for trajectory planning.

In summary, the prototype system delivers AC/PC coordinates as well as the MSP in a fast, and reliable manner. Trajectories for implantation of electrodes are selected self-reliant and assessed objectively for practical use. Used processing times will tremendously speed up pre-operative planning phase. Therefore, the prototypes provide a significant support of the DBS procedure.

References

[1] Krauss J K, Jankovic J, Grossman R G. Surgery for Parkinson's disease and movement disorders. Lippincott Williams and Wilkins, Philadelphia, 2001

[2] Hamani C, Saint-Cyr J A, Fraser J, Kaplitt M, Lozano A M. The subthalamic nucleus in the context of movement disorders. Brain 2003; 127(1):4-20
[3] Benabid A L, Koudsie A, Benazzouz A, Bas J F L, Pollak P. Imaging of subthalamic nucleus and ventralis intermedius of the Thalamus. Movement Disorders 2002; 17(3):123-129
[4] Guridi J, Rodriguez-Oroz M C, Lozano A M, Moro E, Albanese A, Nuttin B, Gybels J, Ramos E, Obeso J A. Targeting the basal ganglia for deep brain stimulation in Parkinson's disease. Neurology 2000; 55(6):21-28
[5] Theodosopulos P V, Marks W J, Christine C W, Starr P A. Locations of movement-related cells in the human subthalamic nucleus in Parkinson's disease. Movement Disorders 2003; 18(7):791-798
[6] Starr P A, Christine C W, Theodosopoulos P V, Lindsey N, Byrd D, Mosley A, Marks W J. Implantation of deep brain stimulators into the subthalamic nucleus: Technical approach and magnetic resonance imaging - Verified lead locations. The Journal of Neurosurgery 2002; 97(2):370-387
[7] Weickert J, ter Haar Romeny B M, Viergever M A. Efficient and reliable schemes for nonlinear diffusion Filtering. IEEE Transactions on Image Processing 1998; 7(3):398-410
[8] Weickert J, Zuiderveld K J, ter Haar Romeny B M, Niessen W J. Parallel implementations of AOS schemes: A fast way of nonlinear diffusion filtering. IEEE International Conference on Image Processing 1997; 3:396-399
[9] Gonzalez R C, Woods R E. Digital image processing. Addison-Wesley Publishing Company 1993; 2
[10] Kass M, Witkin A, Terzopoulos D. Snakes: Active contour models. International Journal of Computer Vision 1988:321-331
[11] Sethian J A. Level set methods and fast marching methods. Evolving Interfaces in Computational Geometry, Fluid Mechanics, Computer Vision and Materials Science, Cambridge University Press 1999
[12] Kahle W, Frotscher M. dtv-Atlas der Anatomie III. Nervensystem und Sinnesorgane. dtv 1997
[13] Otsu N. A threshold selection method from gray-level histograms. IEEE Transactions on Systems, Man, and Cybernetics 1979:62-66